

# Thermal studies on polymorphic structures of tibolone

Gabriel Lima Barros de Araujo · Dalva Lucia Araujo de Faria ·  
Márcio Henrique Zaim · Flávio Machado de Souza Carvalho ·  
Fabio Ramos Dias de Andrade · Jivaldo do Rosario Matos

Received: 21 June 2009 / Accepted: 13 October 2009 / Published online: 2 December 2009  
© Akadémiai Kiadó, Budapest, Hungary 2009

**Abstract** Tibolone polymorphic forms I (monoclinic) and II (triclinic) have been prepared by recrystallization from acetone and toluene, respectively, and characterized by different techniques sensitive to changes in solid state, such as polarized light microscopy, X-ray powder diffractometry, thermal analysis (TG/DTG/DSC), and vibrational spectroscopy (FTIR and Raman microscopy). The nonisothermal decomposition kinetics of the obtained polymorphs were studied using thermogravimetry. The activation energies were calculated through the Ozawa's method for the first step of decomposition, the triclinic form showed a lower  $E_a$  ( $91 \text{ kJ mol}^{-1}$ ) than the monoclinic one ( $95 \text{ kJ mol}^{-1}$ ). Furthermore, Raman microscopy and DSC at low heating rates were used to identify and follow the thermal decomposition of the triclinic form, showing the existence of three thermal events before the first mass loss.

**Keywords** Polymorphism · Solid-state characterization · Thermal decomposition

## Introduction

Tibolone (sometimes abbreviated as Org OD14 or  $7\alpha$ MNa or in full ( $7\alpha,17\alpha$ )-17-hydroxy-7-methyl-19-nor-17-pregn-5(10)-en-20-yn-3-one) is a synthetic steroid (Fig. 1) that is structurally related to the 19 norethisterone derivatives (such as norethynodrel and norethisterone) used to relieve hypo-estrogenic symptoms and protect against bone loss in post-menopausal women. Tibolone has been known since the 1960s, and since the 1980s it has been marketed as Livial [1]. Its preparation was first patented by Organon N. V. in 1965 [2] and published by Wieland and Aner in 1967 [3]. This steroid was later reported by Shouten and Kanters as having the ability to crystallize into two space groups, i.e., to show polymorphism depending on the crystallization solvent [4]. It was found that crystals obtained dissolving tibolone in acetone and pouring the solution into water belong to the monoclinic space group  $P2_1$ , but cooling a hot toluene solution crystals of the triclinic space group  $P1$  were separated.

The conformational analysis of the monoclinic form was published previously by Declercq et al. [5] and polymorphism of tibolone was not mentioned at that time. In the manufacturing process patented in 1990 [6], the two polymorphs were called Form I (monoclinic) and Form II (triclinic). In this patent, further characterization data (diffuse reflectance infrared Fourier transform (DRIFT), X-ray powder diffraction (XRD) and solid-state nuclear magnetic resonance) were briefly presented. It has, moreover, been cited that Form I is chemically appreciably more stable than Form II. According to this patent, this improvement in stability yields great advantages in respect to shelf-life of the pharmaceutical product in which Form I is incorporated [6]. Boerriger et al. extensively studied the relationship between the two polymorphs in terms of their

G. L. B. de Araujo  
Faculdade de Ciências Farmacêuticas, Departamento de  
Farmácia, Universidade de São Paulo, São Paulo, SP, Brazil

D. L. A. de Faria · J. d. R. Matos (✉)  
Departamento de Química Fundamental, Instituto de Química,  
Universidade de São Paulo, São Paulo, SP, Brazil  
e-mail: jdrmatos@gmail.com

M. H. Zaim  
Divisão Hormônios, Sintefina Indústria e Comércio LTDA,  
São Paulo, SP, Brazil

F. M. de Souza Carvalho · F. R. D. de Andrade  
Departamento de Mineralogia e Geotectônica, Instituto de  
Geociências, Universidade de São Paulo, São Paulo, SP, Brazil

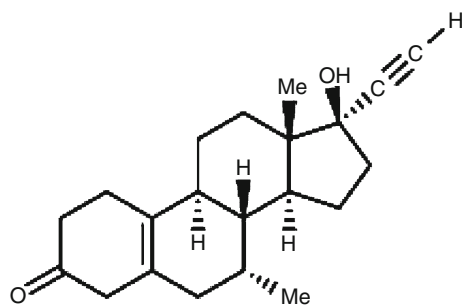


**Fig. 1** Structural formula of tibolone [7, 8]

thermodynamic and kinetic behavior [7]. The authors reported that the triclinic phase can be obtained from apolar solvents like hexane, whereas the monoclinic phase can be obtained from polar media like acetone and acetonitrile; they also concluded that tibolone is an enantiotropic system and that a polymorphic phase transition from the metastable triclinic form to the stable monoclinic can occur in the presence of acetone through a solid–solute–solid mechanism. Furthermore, experimental conditions were found where both polymorphs were grown from the same solvent and at the same temperature, in a concomitant crystallization phenomenon [7].  $^{13}\text{C}$  labeling was used by Booy et al. [8] to enhance the sensitivity of  $^{13}\text{C}$  solid-state NMR to study the effect of tabletting on the polymorphism of tibolone. No changes in crystalline form were observed in that study.

In the present investigation, the solid-state characterization of both polymorphs is performed aiming at to enhance our understanding on tibolone and its thermal behavior.

## Experimental

### Materials and methods

#### Materials

A sample of commercial tibolone at a stated purity of 99.7% was kindly supplied by Sintefina Indústria e Comércio LTDA (Brazil). No attempt was made at further purification. All solvents used were analytical reagent grade or better. Ultra-pure water prepared by reverse osmosis and filtered through 0.45- $\mu\text{m}$  membrane filter was used in all the experiments.

#### Preparation of the samples

**Monoclinic phase: recrystallization from acetone–water** The commercial sample of tibolone was dissolved at 20–25 °C in acetone, to which a trace of pyridine had been

added. The solution was filtered dust-free and the filter was washed with acetone. At a temperature of 15–20 °C, the filtrate was poured as rapidly as possible, under nitrogen, into dust-free distilled water. The suspension was cooled to 0–5 °C and stirred for 1 h at this temperature. The crystals were filtered off, washed with dust-free distilled water, and dried ( $\text{P}_2\text{O}_5$ ) under vacuum in an Abderhalden apparatus.

**Triclinic phase: recrystallization from toluene** The commercial sample of tibolone was dissolved in toluene at 40 °C while stirring vigorously. This solution was allowed to cool down at room temperature spontaneously, after which the mixture was cooled to 0 °C. The crystals were filtered off and washed with toluene at 0 °C. The crystals were dried ( $\text{P}_2\text{O}_5$ ) under vacuum in an Abderhalden apparatus.

#### Characterization of tibolone crystals

**Elemental analysis** Carbon and hydrogen contents were determined by elemental analysis using a PerkinElmer analyzer (Model 2400).

**Optical microscopy** For morphological and optical observations each sample was immersed in an inert colorless mineral oil (Nujol®) on a glass plate, and observed under plane polarized light using a Olympus BX50 microscope. Determination of refractive indexes was made with a set of immersion oils (Argyle) of known refractive indexes

**Scanning electron microscopy (SEM)** Morphology study of crystals was carried out by scanning electron microscopy (SEM) with a Leo Stereoscan 440. Powder samples of tibolone were mounted onto aluminum stubs using double-sided carbon adhesive tape and sputter coated (Baltec Med020 coater) with a thin layer of platinum before examination. The specimens were scanned at low accelerating voltage (10 kV) and the images were collected using secondary electrons detector.

**Raman microscopy** Raman spectra were obtained using laser lines in the visible (632.8 nm) and NIR (1,064 nm). The spectra obtained using the 632.8-nm line were recorded in a Renishaw Raman Microscope (System 3000) consisting of a single spectrograph (0.25-m focal length) containing a holographic grating (1800 grooves  $\text{mm}^{-1}$ ), an Olympus metallurgical microscope and a Peltier-cooled CCD detector ( $600 \times 400$  pixels); the laser line used was from a 35-mW air-cooled He–Ne laser (Spectra Physics, Model 127) and the laser beam was focused on the sample by a  $\times 80$  lens to give a spot size of ca. 4  $\mu\text{m}$ ; the resolution was better than 2  $\text{cm}^{-1}$ .

Excitation in the NIR (1,064 nm) was carried out using a Nd<sup>3+</sup>/YAG laser (Bruker) and the Raman equipment was a FT-Raman Bruker RFS/100, fitted with a liquid N<sub>2</sub> cooled Ge detector. The spectra were recorded with 4 cm<sup>-1</sup> resolution (unless otherwise stated).

**Fourier transform infrared spectroscopy (FTIR)** KBr pellets (3% in mass) of the tibolone crystals were prepared at 20.7 MPa and with a dwell time of 30 s. Sealed liquid cell with 0.025-mm thickness were used to record the spectra from carbon tetrachloride solutions (1 mg mL<sup>-1</sup>). Spectra were recorded on a PerkinElmer Spectrum One FTIR Spectrometer, equipped with a deuterium triglycine sulfate (DTGS) detector. The scan speed was set at 0.5 cm s<sup>-1</sup>. Baseline was corrected for all spectra using the PerkinElmer Spectrum software. Each spectrum resulted from 16 single averaged scans collected in the 450–4,000 cm<sup>-1</sup> region at a spectral resolution of 4 cm<sup>-1</sup>. Attenuated total reflectance Fourier transform infrared (ATR FTIR) spectra of tibolone monoclinic and triclinic samples in the 650–4,000 cm<sup>-1</sup> range were obtained using a single reflection horizontal ATR accessory (PerkinElmer Miracle SR ATR Spectrum One, fitted with a ZnSe crystal).

**X-ray powder diffraction (XRD)** X-Ray powder diffraction patterns were recorded in a Siemens/Bruker D5000, using: Ni filtered Cu K $\alpha$  radiation ( $\lambda = 1.5418 \text{ \AA}$ ) at high voltage (40 kV) and tube current of 40 mA, step size of 0.02°, step time 5 s with angular range  $5^\circ < (2\theta) < 90^\circ$ .

**Thermal analysis** Differential scanning calorimetry (DSC) curves were obtained in a DSC-50 cell (Shimadzu) using aluminum crucibles with about 2 mg of samples, under dynamic N<sub>2</sub> atmosphere (50 mL min<sup>-1</sup>) and heating rate of 10 or 2 °C min<sup>-1</sup> in the temperature range from 25 to 600 °C. The DSC cell was calibrated with indium (mp 156.60 °C;  $\Delta H_{\text{fus}} = 28.62 \text{ J g}^{-1}$ ) and zinc (mp 419.53 °C;  $\Delta H_{\text{fus}} = 108.09 \text{ J g}^{-1}$ ). Specific heat was determined in the same equipment with Specific Heat Capacity TA-50 software version 1.02 using Al<sub>2</sub>O<sub>3</sub> as the reference material. Thermogravimetry/Derivative thermogravimetry

(TG/DTG) curves were obtained with a thermobalance model TGA 50 (Shimadzu) in the temperature range 25–900 °C using platinum crucibles with ~5 mg of sample, under dynamic nitrogen atmosphere (50 mL min<sup>-1</sup>) and heating rate of 10 or 2 °C min<sup>-1</sup>. The determination of kinetic parameters for the first thermal decomposition step of the samples was carried out by applying the Ozawa's method [9, 10] in which the slope of the log (heating rate) versus 1/T plot gives the activation energy ( $E_a$ ) of the process. In this work, the heating rates used were 2.5, 5.0, 7.5, 15.0, and 20.0 °C min<sup>-1</sup>. The kinetic parameters were obtained using the Tasys Shimadzu software.

## Results and discussion

### Elemental analysis

Chemical composition expressed as %C and %H for both crystalline phases are (a) from toluene: C = 80.85 and H = 9.00 wt%; (b) from acetone: C = 80.60 and H = 9.10 wt%. These results are in full agreement with the literature data (C = 80.73 and H = 9.03 wt%) [11].

### Microscopy

Optical properties of the samples are summarized in Table 1. All analyzed samples analyzed present birefringence (optical anisotropy), which is indicative of their non-isometric crystalline state. SEM and polarized light micrographs of the samples are shown in Fig. 2. The minute crystal size of the samples and their platy to bladed crystal habit preclude precise determination of all refractive indexes. Regarding the optical indicatrix of both polymorphs, the identification of their biaxial character—i.e., the presence of two optical axes, which are directions in which the light does not undergo double refraction—indicates that the two polymorphs belong to the orthorhombic, monoclinic, or triclinic crystal systems, ruling out the hexagonal, trigonal, and tetragonal systems. The pinacoidal habit observed in the two polymorphs, lacking a symmetry axis, is indicative of monoclinic and triclinic

**Table 1** Microscopy characterization data of tibolone crystals: crystal grown from acetone (ACE) and crystal grown from toluene (TOLU); n.d. = not determinate

Refractive indexes								
Sample	Crystal forms/habit	Minimum n $\alpha$	Intermediated n $\beta$	Maximum n $\gamma$	Birrefrigence (Δ)	2V/ $^{\circ}$	Optical signal	System
ACE	Tabular. platy. pinacoids {100}. {010}.{001}	1.570	n.d	1.610	0.040	n.d	n.d	Monoclinic
TOLU	Bladed pinacoidal	1.552(5)	1.592(5)	1.640(5)	0.088(5)	85–90(5)	2Vz (+)	Triclinic

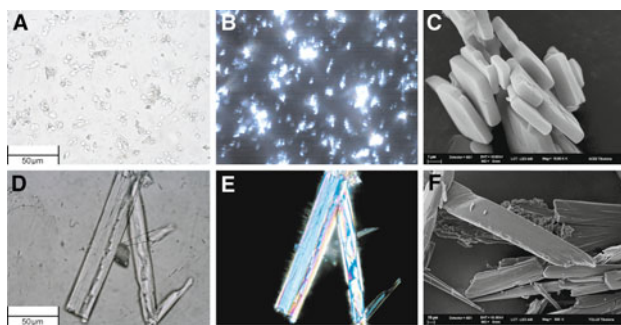


**Fig. 2** Optical micrographs ( $\times 50$ ) of tibolone crystals: obtained from acetone with unpolarized (a) and polarized light (b); obtained from toluene with unpolarized (d) and polarized light (e). SEM micrographs of tibolone crystals: obtained from acetone 10000X (c); obtained from toluene 700X (f)

systems. Distinction between these two systems based only on their optical properties is not straightforward, particularly in small size crystals. Hence, optical microscopy was supported by XRD in order to distinguish between monoclinic and triclinic polymorphs. It was possible to show that the birefringence of the triclinic form is twice that of the monoclinic.

In our experiments, the stable monoclinic form of tibolone obtained from acetone displays a bladed to platy habit (Fig. 2c), similar to those obtained from Stoica et al. [11, 12], while the triclinic form, obtained from toluene, displays a rather prismatic crystalline habit instead of a massive, irregular or chunky habit already described for triclinic crystals formed from toluene [13]; the latter crystals have irregular surfaces and corrugated edges (Fig. 2f).

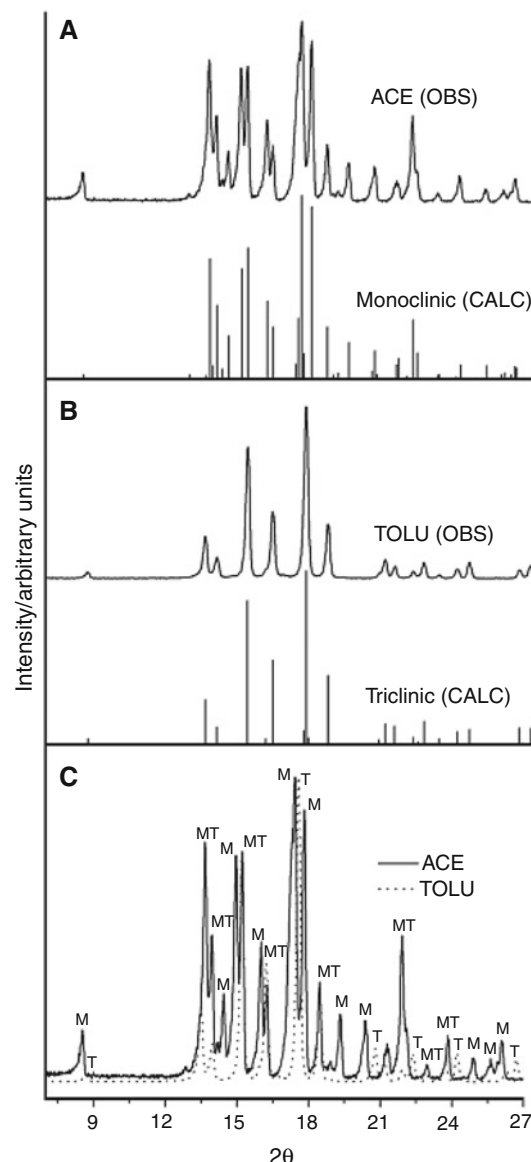
#### X-Ray powder diffraction

Figure 3 presents the experimental XRD patterns of tibolone crystals prepared from acetone and toluene, as well as the calculated diffractogram using the reported structural parameters for monoclinic [5] and triclinic [4] systems. Powder-diffraction data are listed in Table 2 with the characteristic diffraction peaks assigned in Fig. 3c. The XRD patterns are in good agreement with the reported calculated patterns [4, 5].

#### Fourier transform infrared spectroscopy (FTIR)

Figure 4a presents the FTIR spectra of both samples dissolved in  $\text{CCl}_4$ . The spectra confirm that the chemical composition of the two tibolone samples is the same.

Potassium bromide pellet method was also employed to evaluate possible polymorphic transition eventually produced during sampling, caused by pressure and solid solution effects in the crystal spectra. All FTIR spectra of crystals, recorded as KBr pellets and using ATR accessory, are similar



**Fig. 3** Experimental (OBS) and calculated (CALC) XRD patterns for tibolone crystal forms: **a** crystals from acetone (ACE) and calculated pattern for the monoclinic phase [5]; **b** crystals from toluene (TOLU) and calculated pattern for the triclinic phase [4]; **c** overlay of experimental XRD data (M—monoclinic phase; T—triclinic phase)

to those previously reported for polymorphs I and II by DRIFT spectroscopy (DRIFTS) [6]. However, the spectra from KBr pellets present broader bands and shoulders when compared with those recorded by the ATR technique, indicating that changes in crystal structure may occur as a result from extensive grinding and compression (Fig. 4b).

In the  $3200\text{--}3450\text{ cm}^{-1}$  region of the ATR spectra (Fig. 4c), the  $3,265$  and  $3,489\text{ cm}^{-1}$  bands in the triclinic form are attributed to  $\equiv\text{C-H}$  and OH stretching, respectively. In the monoclinic form spectra, those bands are splitted at  $3,251/3,270\text{ cm}^{-1}$  ( $\equiv\text{C-H}$ ) and  $3,407/3,488\text{ cm}^{-1}$  (OH) bands.

**Table 2** Comparison of observed and calculated X-ray diffraction data of tibolone crystals

Monoclinic (calc)			Triclinic (calc)			ACE (obs)			TOLU (obs)		
2 $\theta$ <sup>a</sup>	d-Space/Å	Rel. int./% <sup>b</sup>	2 $\theta$ <sup>a</sup>	d-Space/Å	Rel. int./% <sup>b</sup>	2 $\theta$ <sup>a</sup>	d-Space/Å	Rel. int./% <sup>b</sup>	2 $\theta$ <sup>a</sup>	d-Space/Å	Rel. int./% <sup>b</sup>
8.58	10.30	0.65	—	—	—	8.52	10.38	17.61	—	—	—
—	—	—	8.72	10.13	2.82	—	—	—	8.70	10.16	4.45
12.88	6.87	0.90	—	—	—	—	—	—	—	—	—
—	—	—	13.49	6.56	25.47	—	—	—	13.48	6.57	25.12
13.53	6.54	1.65	—	—	—	—	—	—	—	—	—
13.70	6.46	65.61	—	—	—	13.66	6.48	78.82	—	—	—
13.81	6.41	7.20	—	—	—	—	—	—	—	—	—
—	—	—	13.96	6.34	9.85	—	—	—	13.96	6.34	13.22
13.98	6.33	40.07	—	—	—	13.96	6.34	48.48	—	—	—
—	—	—	—	—	—	14.16	6.25	13.26	—	—	—
14.20	6.23	5.44	—	—	—	14.22	6.23	13.75	—	—	—
14.47	6.12	23.24	—	—	—	14.44	6.13	29.35	—	—	—
14.99	5.91	59.69	—	—	—	14.96	5.92	74.43	—	—	—
—	—	—	15.20	5.82	82.87	—	—	—	15.22	5.82	76.58
15.25	5.81	71.46	—	—	—	15.22	5.82	75.22	—	—	—
—	—	—	15.94	5.56	2.91	—	—	—	16.02	5.53	7.67
16.04	5.52	42.27	—	—	—	16.02	5.53	46.31	—	—	—
—	—	—	16.23	5.46	48.30	16.22	5.46	28.82	16.22	5.46	39.33
16.28	5.44	28.25	—	—	—	16.26	5.45	32.35	16.26	5.45	36.38
17.20	5.15	8.03	—	—	—	—	—	—	—	—	—
17.29	5.12	7.68	—	—	—	—	—	—	—	—	—
17.30	5.12	33.09	—	—	—	17.30	5.13	78.78	—	—	—
17.43	5.08	100.00	—	—	—	17.42	5.09	100.00	—	—	—
—	—	—	17.49	5.07	7.50	—	—	—	—	—	—
17.52	5.06	13.95	—	—	—	—	—	—	—	—	—
—	—	—	17.59	5.04	100.00	—	—	—	17.60	5.04	100.00
—	—	—	17.68	5.01	3.30	—	—	—	—	—	—
17.83	4.97	93.93	—	—	—	17.82	4.98	89.25	—	—	—
18.47	4.80	28.34	18.47	4.80	39.52	18.48	4.80	29.68	18.48	4.80	31.90
18.72	4.74	2.07	—	—	—	—	—	—	—	—	—
18.93	4.69	3.18	—	—	—	—	—	—	—	—	—
19.33	4.59	19.69	—	—	—	19.32	4.59	22.66	—	—	—
20.28	4.38	4.30	—	—	—	—	—	—	—	—	—
20.40	4.35	15.24	—	—	—	20.36	4.36	20.73	—	—	—
20.47	4.34	2.23	—	—	—	—	—	—	—	—	—
—	—	—	20.54	4.32	2.55	—	—	—	—	—	—
—	—	—	20.80	4.27	11.38	—	—	—	20.80	4.27	11.59
—	—	—	21.18	4.19	10.31	—	—	—	21.20	4.19	7.71
21.26	4.18	7.55	—	—	—	21.20	4.19	10.22	—	—	—
21.37	4.15	11.13	—	—	—	21.28	4.18	12.97	—	—	—
21.55	4.12	0.18	—	—	—	—	—	—	—	—	—
21.62	4.11	0.49	—	—	—	—	—	—	—	—	—
21.70	4.09	1.62	—	—	—	—	—	—	—	—	—
—	—	—	—	—	—	21.92	4.05	48.36	21.92	4.05	4.49
—	—	—	21.94	4.05	3.78	21.94	4.05	43.27	21.94	4.05	4.77
21.95	4.05	31.97	—	—	—	—	—	—	—	—	—
22.12	4.01	14.18	—	—	—	—	—	—	—	—	—

**Table 2** continued

Monoclinic (calc)			Triclinic (calc)			ACE (obs)			TOLU (obs)		
2 $\theta$ <sup>a</sup>	d-Space/Å	Rel. int./%	2 $\theta$ <sup>a</sup>	d-Space/Å	Rel. int./%	2 $\theta$ <sup>a</sup>	d-Space/Å	Rel. int./%	2 $\theta$ <sup>a</sup>	d-Space/Å	Rel. int./%
–	–	–	22.13	4.01	1.07	–	–	–	–	–	–
22.24	3.99	0.10	–	–	–	22.36	3.98	2.34	–	–	–
22.96	3.87	2.01	–	–	–	22.94	3.88	6.32	–	–	–
–	–	–	22.98	3.87	3.02	–	–	–	22.98	3.87	2.74
22.99	3.86	2.24	–	–	–	22.98	3.87	5.21	–	–	–
23.70	3.75	0.88	–	–	–	23.72	3.75	7.27	–	–	–
–	–	–	23.73	3.75	7.03	–	–	–	23.72	3.75	6.35
23.87	3.73	5.80	–	–	–	23.82	3.74	15.89	–	–	–
23.87	3.72	7.52	–	–	–	–	–	–	–	–	–
–	–	–	24.22	3.67	8.40	–	–	–	24.24	3.67	10.04
24.49	3.63	0.54	–	–	–	–	–	–	–	–	–
24.94	3.57	7.14	–	–	–	24.88	3.58	8.46	–	–	–
25.53	3.49	2.08	–	–	–	25.28	3.52	1.81	–	–	–
25.68	3.47	3.28	–	–	–	25.62	3.48	8.17	–	–	–
25.92	3.43	1.99	–	–	–	–	–	–	–	–	–
26.08	3.41	6.63	–	–	–	26.08	3.42	14.16	–	–	–
26.14	3.41	5.74	–	–	–	26.26	3.39	2.34	–	–	–
–	–	–	26.23	3.39	9.39	–	–	–	26.08	3.42	1.35
–	–	–	26.37	3.38	0.43	–	–	–	26.26	3.39	5.48
–	–	–	26.70	3.34	9.03	–	–	–	26.70	3.34	8.22

<sup>a</sup> CuK $\alpha$  radiation ( $\lambda = 1.5418 \text{ \AA}$ )<sup>b</sup> Relative intensity (Rel. int./%) is calculated by dividing the intensity of the peak at the indicated angle by the intensity of the highest peak and multiplying by 100

The splitting of bands arises from the conformational differences described by Declercq et al. [5] and also noticed by Boerrigter et al. [7] in the Raman spectra of each polymorph. According to the authors, the monoclinic form consists of two steroid conformers mainly differing in the adjacent carbonyl holding ring (ring A, Fig. 1), which can exist in two-half-chair conformations [7]. The monoclinic form may present both conformations, whereas the triclinic form only present one conformation [4, 5]. These differences in the spectra show the influence of lattice arrangement in polymorphism studies which can affect different regions of vibrational spectra. No strong hydrogen bonds are present in the crystal structure of tibolone crystals according to the IR spectral data obtained, since no broad and intense absorption was observed in the considered spectral window (3,200–3,500 cm<sup>-1</sup>).

#### Raman microscopy

Raman spectra of triclinic and monoclinic tibolone excited at 632.8 nm are shown in Fig. 4d. The spectral window 1,600–1,800 cm<sup>-1</sup> were chosen according to differences

reported by Boerrigter et al. [7]. The triclinic form shows only two bands in the 1,600–1,800 cm<sup>-1</sup> region (1,661 and 1,715 cm<sup>-1</sup>). The 1,715 cm<sup>-1</sup> band is assigned to a carbonyl stretching vibration and the 1,661 cm<sup>-1</sup> band to a C=C (carbon 5 and 10, Fig. 1) stretching vibration. The monoclinic phase can be differentiated by the splitting of the C=C vibration at 1,657/1,664 cm<sup>-1</sup> due to the conformational differences already cited. The carbonyl band in the monoclinic structure shows a shift to 1,710 cm<sup>-1</sup>, what can also be used for differentiation purposes.

#### Thermal analysis

The thermoanalytical profiles obtained using heating rate at 10 °C min<sup>-1</sup> for monoclinic and triclinic samples of tibolone are presented in Fig. 5a. The TG/DTG curves in dynamic nitrogen atmosphere indicate that the thermal decomposition process of triclinic tibolone crystals occurs in three stages in the following temperature range and respective weight loss: 180–350 °C ( $\Delta m_1 = 24.2\%$ ), 350–530 °C ( $\Delta m_2 = 60.5\%$ ), and 530–790 °C ( $\Delta m_3 = 14.7\%$ ). For monoclinic crystals, the thermal decomposition process occurs in three stages in

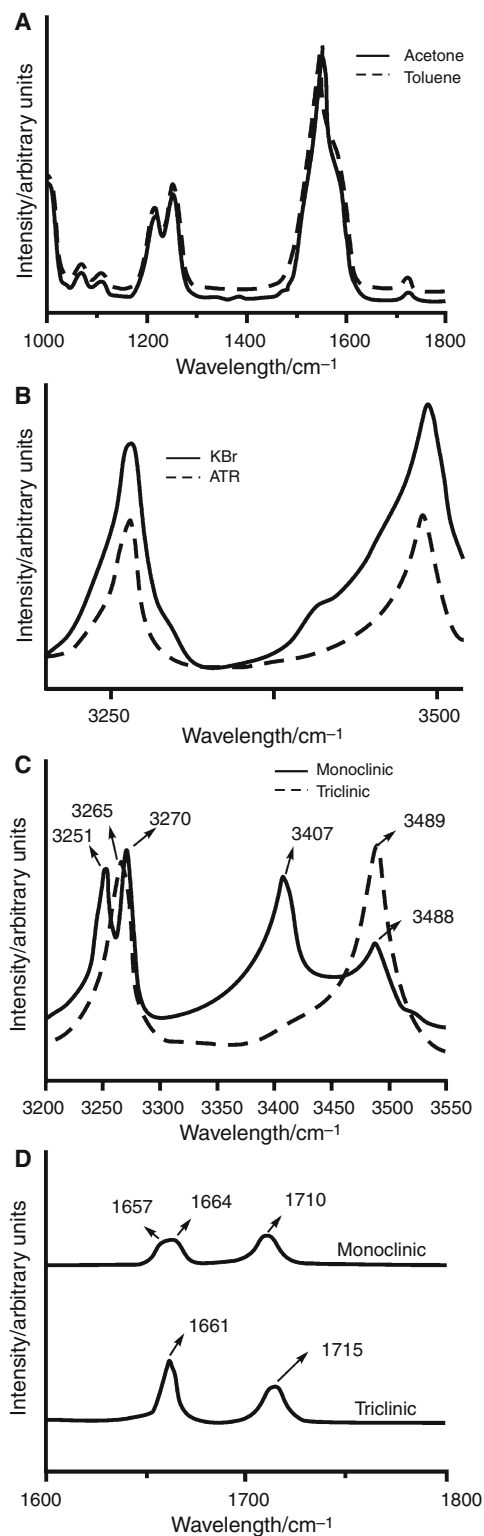


**Fig. 4** Vibrational spectra of tibolone crystal forms: **a** FTIR spectrum of  $\text{CCl}_4$  solution of the samples obtained from acetone (monoclinic) and from toluene (triclinic). **b** Comparison between ATR and KBr pellet FTIR spectrum of the triclinic sample. **c** Overlay of the FTIR/ATR spectrum of monoclinic and triclinic samples of tibolone. **d** Raman spectra of triclinic and monoclinic tibolone (excited at 632.8 nm)

the following temperature range and weight loss: 185–360 °C ( $\Delta m_1 = 56.8\%$ );  $\Delta m_2 = 360$ –500 °C (36.6%);  $\Delta m_3 = 500$ –790 °C (6.5%). These thermal decomposition data suggest a higher decomposition rate for the monoclinic crystals. In both forms, no significant thermal decomposition (weight loss) was observed during the melting process.

Even though, experiments in dynamic nitrogen atmosphere have shown differences in the thermal decomposition profiles of tibolone crystal forms. Thermogravimetric experiments at  $10 \text{ }^\circ\text{C min}^{-1}$  in dynamic air atmosphere (Fig. 5c) produced similar curves from both samples as a result of a complete combustion reaction.

The method established by Ozawa by non-isothermal TG [9, 10] was used for the activation energy ( $E_a$ ) determination of the first decomposition step (Fig. 5c, d). Table 3 summarizes the kinetics data. The triclinic sample showed a lower  $E_a$  ( $91 \text{ kJ mol}^{-1}$ ) than the monoclinic one ( $95 \text{ kJ mol}^{-1}$ ). Even considering that the difference between  $E_a$  is small, the thermogravimetric profiles show that after melting the specimens present are different since they decompose following distinct mechanisms which is also indicated by frequency and order of reaction data.

DSC profiles for monoclinic and triclinic tibolone samples obtained at a heating rate of  $10 \text{ }^\circ\text{C min}^{-1}$  are shown in Fig. 5b. Monoclinic form melts at  $169 \text{ }^\circ\text{C}$  ( $\Delta H_{\text{melt}} = 29.8 \text{ kJ mol}^{-1}$ ;  $T_{\text{peak}} = 171 \text{ }^\circ\text{C}$ ) with no other phase transition before this event. For triclinic form, it can be seen that at this heating rate a single endothermic transition with an  $T_{\text{onset}}$  at about  $148 \text{ }^\circ\text{C}$  ( $\Delta H_{t1} = 21.0 \text{ kJ mol}^{-1}$ ;  $T_{\text{peak}} = 158 \text{ }^\circ\text{C}$ ) followed by a second weak endothermic event at  $163 \text{ }^\circ\text{C}$  ( $\Delta H_{t2} = 3.0 \text{ kJ mol}^{-1}$ ;  $T_{\text{peak}} = 166 \text{ }^\circ\text{C}$ ). These values are comparable with those two transitions reported previously for this polymorph at  $5 \text{ }^\circ\text{C min}^{-1}$  [7]. However, the first event presents a peak with shoulder ( $T_{\text{peak}} = 152 \text{ }^\circ\text{C}$ ) indicating an overlay of events. The first derivative curve (DDSC not shown) clearly indicates that two events occur.

#### Thermal events studies

In order to separate the thermal events observed for the triclinic crystal, new DSC experiments were carried out at  $2 \text{ }^\circ\text{C min}^{-1}$  (Fig. 6a). At this heating rate, it was possible to observe three thermal events between 140 and 170 °C instead of the two described in literature [7]. Thermoanalytical data of those events are present in Table 4.

For a better understanding of those events, samples I, II, and III were collected after the occurrence of each thermal event showed on the curve DSC at 150, 158, and 170 °C, respectively. These samples were analyzed by Raman microscopy and the spectra are shown in Fig. 6b.

**Fig. 5** Thermoanalytical profiles for monoclinic and triclinic samples of tibolone: **a** TG/DTG curves obtained in dynamic nitrogen atmosphere ( $50 \text{ mL min}^{-1}$ ) and heating rate  $10 \text{ }^{\circ}\text{C min}^{-1}$ ; **b** DSC curves obtained in dynamic nitrogen atmosphere ( $50 \text{ mL min}^{-1}$ ) and heating rate  $10 \text{ }^{\circ}\text{C min}^{-1}$ ; **c** TG curves obtained in dynamic air atmosphere ( $50 \text{ mL min}^{-1}$ ) and heating rate  $10 \text{ }^{\circ}\text{C min}^{-1}$ ; overlay of monoclinic (**d**) and triclinic (**e**) TG curves obtained in dynamic nitrogen atmosphere ( $50 \text{ mL min}^{-1}$ ) at different heating rate in the kinetics study

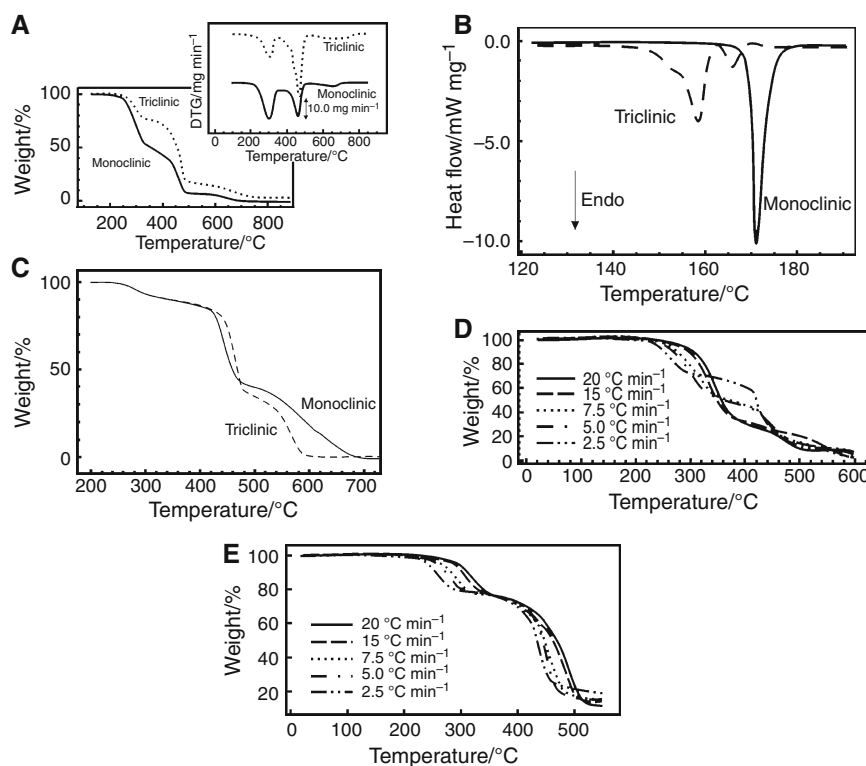


**Table 3** Kinetic parameters for the thermal decomposition of the monoclinic and triclinic tibolone obtained from dynamic TG measurements

Crystal	DTG peak 1	$E_a/\text{kJ mol}^{-1}$	Factor frequency	Reaction order
Monoclinic	295	95	$1.02 \times 10^8$	1.0
Triclinic	289	91	$1.82 \times 10^7$	2.0

The Raman spectra show no evidence of phase transition from triclinic to monoclinic form but only a continuous tendency of I and II spectra toward the melted sample III spectrum. The spectra of pure triclinic and monoclinic polymorphs show no shift at  $1,620$  and  $1,608 \text{ cm}^{-1}$  as presented by the heated samples indicating the formation of a new chemical species. Also an yellowish color can be noticed in all the heated samples (I, II, and III). It can thus be concluded that during melting thermal degradation is very likely to be the most probable thermal event observed in the DSC curves of the triclinic crystals. It is important to remark that TG/DTG curves do not show weight loss at the temperature of the events, indicating no release of volatiles and probably only the formation of new species, the non-identified thermal degraded compound.

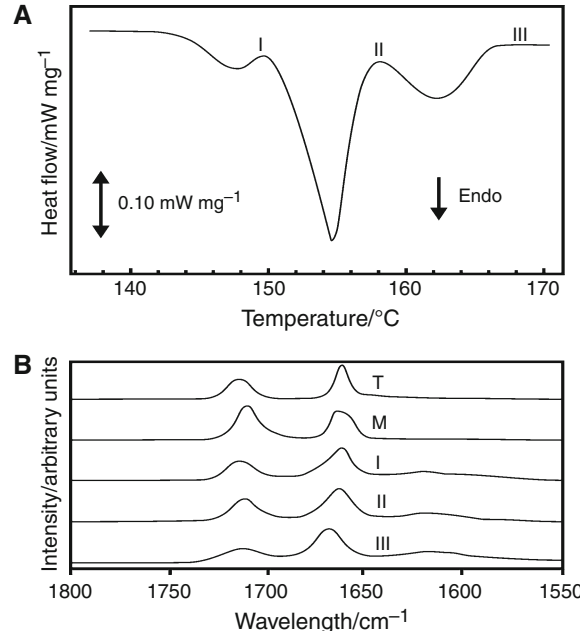


**Fig. 6** Study of thermal events observed for the triclinic crystal of tibolone: **a** DSC curves of triclinic tibolone obtained in dynamic nitrogen atmosphere ( $50 \text{ mL min}^{-1}$ ) at  $2 \text{ }^{\circ}\text{C min}^{-1}$  (I, II, and III refers to samples of at  $150$ ,  $158$ , and  $170 \text{ }^{\circ}\text{C}$ , respectively). **b** Comparison between Raman spectra of the residues collected (I, II, and III) and monocrystalline (*M*) and triclinic (*T*) tibolone

**Table 4** Thermodynamic data for triclinic tibolone crystals events observed in the DSC curves obtained in dynamic nitrogen atmosphere ( $50 \text{ mL min}^{-1}$ ) at  $2 \text{ }^{\circ}\text{C min}^{-1}$ 

Data	First event	Second event	Third event
$T_{\text{onset}}/{}^{\circ}\text{C}$	145	152	159
$\Delta H_i/\text{kJ mol}^{-1}$	0.90	6.5	2.0
$T_{\text{peak}}/{}^{\circ}\text{C}$	148	155	162

## Conclusions

Tibolone crystallized from toluene and acetone was characterized by polarized light microscopy, SEM, X-ray powder diffractometry, thermal analysis (TG/DSC), IR, and Raman spectroscopy. All the experimental results indicate the presence of triclinic and monoclinic forms of the synthetic steroid.

Also overlapped thermal events on DSC curves were observed for triclinic crystal and not observed for monoclinic crystal, which presents only a single melt peak. Those events were separated by using lower heating rates in the DSC experiments. Raman spectra of the triclinic sample after heating indicate that a new specimen formation occurs with no evidence of phase transition. However, no weight loss is show by TG/DTG curves at that temperature range. This fact could explain the different thermal degradation kinetics behavior between monoclinic and triclinic samples, since different specimens are present after the melting for both polymorphs resulting in different TG curves for each polymorph. Further studies should be carried out in order to characterize the degradation product, evaluate the nature of those thermal events and compare the pharmaceutical stability of tibolone polymorphs in formulated products.

**Acknowledgements** The authors would like to thank Professor José Moacyr Vianna Coutinho for his kind help with the microscopy experiments and Sintefina Indústria e Comércio LTDA for kindly providing the starting material. The authors acknowledge also Conselho Nacional de Desenvolvimento Científico e Tecnológico (CNPq)

and the Fundação de Amparo à Pesquisa do Estado de São Paulo (FAPESP).

## References

- Rymer J. Why tibolone is different? *Rev Gynaecol Pract.* 2002;2: 165–70.
- Organon NV. 7-Methylestrenes. 6 pp; 1965. NL 6406797 19651217 Application: NL 19640615. Priority: NL 19640615. CAN 64:68087 AN 1966:68087.
- Wieland P, Anner G. Steroids. Synthesis of 7alpha-methyl-3-oxo-19-norandrosta-4, 9, 11-trienes. *Helv Chim Acta.* 1967;50(6): 1453–61.
- Schouten A, Kanters JA. Structure of the triclinic modification of  $17\beta$ -hydroxy-19-nor-7 $\alpha$ -methyl-17 $\alpha$ -pregn-5(10)-en-20-in-3-one (Org OD 14). *Acta Crystallogr C.* 1991;47:1754–6.
- Declercq JP, Van Meerssche M, Zeelen FJ. Conformational analysis of 3-oxo 5(10)-unsaturated steroids. Single-crystal X-ray structure analysis of 17-hydroxy-7 $\alpha$ -7-pregn-5(10)-en-20-in-3-one (Org OD 14). *Recl Trav Chim Pays Bas.* 1984;103:145–7.
- Sas GAJMT, Van Doornum EM. Pharmaceutical composition which contains a pharmaceutically suitable carrier and the compound having the structure (7 alpha, 17 alpha)-17-hydroxy-7-methyl-19-nor-17-pregn-5(10)-en-20-yn-3-one. EP Pat. 0 389 035; 1990.
- Boerrigter SXM, Van Den Hoogenhof CJM, Meekes H, Bennema P, Vlieg E. In situ observation of epitaxial polymorphic nucleation of the model steroid methyl analogue 17 norethindrone. *J Phys Chem B.* 2002;106:4725–31.
- Booy K, Wiegerinck P, Vader J, Kaspersen F, Lambregts D, Vromans H, et al. The use of  $^{13}\text{C}$  labeling to enhance the sensitivity of  $^{13}\text{C}$  solid-state CPMAS NMR to study polymorphism in low dose solid formulations. *J Pharm Sci.* 2005;94(2):458–63.
- Ozawa T. A new method of analyzing thermogravimetric data. *J Bull Chem Soc Jpn.* 1965;38(11):1881–6.
- Felix FS, Cides da Silva LC, Angnes L, Matos JR. Thermal behavior study and decomposition kinetics of salbutamol under isothermal and non-isothermal conditions. *J Therm Anal Calorim.* 2009;95(3):877–80.
- Budavari S, editor. The Merck index. 11th ed. N.J.: Rahway; 1989. p. 1485.
- Stoica C, Tinnemans P, Meekes H, Vlieg E. Epitaxial 2D nucleation of metastable polymorphs: a 2D version of Ostwald's rule of stages. *Cryst Growth Des.* 2005;5(3):975–81.
- Stoica C, Verwer P, Meekes H, Vlieg E, Van Hoof PJCM, Kaspersen FM. Epitaxial 2D nucleation of the stable polymorphic form of the steroid 7MNa on the metastable form: Implications for Ostwald's rule of stages. *Int J Pharm.* 2006;309(1–2):16–24.